2021

End-Effector Contact and Force Detection for Miniature Autonomous Robots Performing Lunar and Expeditionary Surgery

Eric T. Psota

Jay Carlson

Priscila Rodrigues Armijo

Laura Flores

Ka-Chun Siu

See next page for additional authors

Authors
Eric T. Psota, Jay Carlson, Priscila Rodrigues Armijo, Laura Flores, Ka-Chun Siu, Dmitry Oleynikov, Shane Farritor, and Nathan Bills

End-Effector Contact and Force Detection for Miniature Autonomous Robots Performing Lunar and Expeditionary Surgery

Eric Psota, PhD[,†]; Jay Carlson, PhD Scholar[†]; Priscila Rodrigues Armijo, M.D.[*,‡]; Laura Flores, BA[*]; Ka-Chun Siu, PhD[*,§]; Dmitry Oleynikov, MD[‖]; Shane Farritor, PhD[‖,¶]; Nathan Bills, PhD, MBA[*,‡]*

ABSTRACT

Introduction:

The U.S. Space Force was stood up on December 20, 2019 as an independent branch under the Air Force consisting of about 16,000 active duty and civilian personnel focused singularly on space. In addition to the Space Force, the plans by NASA and private industry for exploration-class long-duration missions to the moon, near-earth asteroids, and Mars makes semi-independent medical capability in space a priority. Current practice for space-based medicine is limited and relies on a "life-raft" scenario for emergencies. Discussions by working groups on military space-based medicine include placing a Role III equivalent facility in a lunar surface station. Surgical capability is a key requirement for that facility.

Materials and Methods:

To prepare for the eventuality of surgery in space, it is necessary to develop low-mass, low power, mini-surgical robots, which could serve as a celestial replacement for existing terrestrial robots. The current study focused on developing semi-autonomous capability in surgical robotics, specifically related to task automation. Two categories for end-effector tissue interaction were developed: Visual feedback from the robot to detect tissue contact, and motor current waveform measurements to detect contact force.

Results:

Using a pixel-to-pixel deep neural network to train, we were able to achieve an accuracy of nearly 90% for contact/no-contact detection. Large torques were predicted well by a trained long short-term memory recursive network, but the technique did not predict small torques well.

Conclusion:

Surgical capability on long-duration missions will require human/machine teaming with semi-autonomous surgical robots. Our existing small, lightweight, low-power miniature robots perform multiple essential tasks in one design including hemostasis, fluid management, suturing for traumatic wounds, and are fully insertable for internal surgical procedures. To prepare for the inevitable eventuality of an emergency surgery in space, it is essential that automated surgical robot capabilities be developed.

INTRODUCTION

Human exploration throughout our solar system has long been a priority for NASA and has recently gained attention in private industry. Research and development priorities have expanded to include long-duration missions to the moon, near-earth asteroids, and Mars. These momentous pursuits have also been joined with the new Space Force. The Space Force, the first new military service in more than 70 years, is intended to serve as the lead military service for space operations and consists of ∼16,000 personnel.[1] As we aspire to the goal of long-term space missions, it is imperative for NASA, the Space Force, and private industry to address sustained medical capacity for long-term space missions.

Surgery performed at a distance, telesurgery or telepresence surgery, has been a topic of research for over 25 years.[2,3] This early research investigated robotics for telesurgery for forward military applications. The idea was that a robot could be deployed in a high-risk environment, such as a battlefield, and surgery could be performed by a surgeon in a remote and safe location. This work led to the development of the da Vinci Surgical System that has now become the standard of care for several procedures [e.g., 3].[4]

[*]Center for Advanced Surgical Technology, 986245 Nebraska Medical Center, Omaha, NE, 69818-6245, USA

[†]Department of Electrical and Computer Engineering, University of Nebraska-Lincoln, Lincoln, NE, 68588-0511, USA

[‡]Department of Surgery, University of Nebraska Medical Center, 986246 Nebraska Medical Center, Omaha, NE, 69818-6245, USA

[§]College of Allied Health Professions, University of Nebraska Medical Center, 984420 Nebraska Medical Center, Omaha, NE, 69818-4220, USA

[‖]Virtual Incision Corporation, Lincoln, NE, 68508, USA

[¶]Department of Mechanical and Material Engineering, University of Nebraska-Lincoln, Lincoln, NE 68588-0526, USA

Presented as a poster at the 2019 Military Health System Research Symposium, Kissimmee, FL; MHSRS-19-02379.

The views expressed in this paper are those of the authors and do not necessarily represent the official position or policy of the U.S. Government, the Department of Defense, or the Department of the Air Force. Dr. Dmitry Oleynikov and Dr. Shane Farritor disclose that they are stockholders in Virtual Incision Corporation.

doi:10.1093/milmed/usaa443

Other research has investigated different types of robot system that are smaller and more easily deployed to remote environments and can also be assistants in surgical systems.[5,6] The most extensive research was a DARPA project called Trauma Pod that sought to make a fully autonomous system for surgery in remote environments.[7] Trauma Pod attempted to automate some aspects of surgery so that less trained personnel, such as an astronaut, could be more capable in the forward environment. Other research focused on the automation of specific surgical tasks such as suturing.[8]

Specific to surgery in space, some work has investigated using "aqueous immersion" as a means of controlling bleeding during surgery in micro-gravity.[9] Using a fluid to apply pressure to the surgical environment could prevent blood from becoming free in the operating room. This work further progressed into the creation of a chamber for this type of surgery.[10]

Current practice for space-based medicine is limited. Although our understanding of the consequences of long-term space exploration is growing, the strategies for responding to medical emergencies in space are still incomplete.[11] Currently, the response to medical emergencies on the space station relies on a "life-raft" scenario, where an injured astronaut would be returned to earth as quickly as possible on available craft.[12] Although areas including diagnostic evaluation, hemorrhage control, and the effects of microgravity have been explored; more research and development is needed particularly in terms of urgent extra-terrestrial surgical treatment and medical care systems.[13,14] To address this gap, current discussions for space-based medicine include placing a Role III equivalent medical facility on a lunar surface station. Role III equivalent facilities must have the capability for general and subspecialty surgical procedures, and we believe a key requirement for in-flight expeditionary medical care would be a surgical robotic system.[14] It has been established that minimally invasive surgical procedures, such as laparoscopy and thoracoscopy, are possible in a microgravity environment.[15] Other groups have also demonstrated the feasibility of advanced trauma life support procedures performed during parabolic flights.[16] Additionally, diagnostic capabilities, even if limited to ultrasonography, currently exist, with the cumulative knowledge of the physiologic variations in this environment.[14,15] However, this still does not address the challenges of communication delay between crew and Earth, nor the need for trained personnel to perform these complex procedures on-site.[14,17]

Telesurgery has long been contemplated as a technical solution to solve the issue of a lack of proximate skilled surgical expertise. Indeed, the original vision for development of telesurgical robots by DARPA (leading eventually to the daVinci robot) was for remote surgeons to operate in the battlefield with a mobile surgical unit linked via two-way microwave communication.[18] The first transcontinental surgery (a cholecystectomy) was performed in 2001.[19] Steady improvements in bandwidth and reliability have sped the subsequent adoption of telesurgery. Anvari et al. (2005) documented a fully implemented remote telesurgical network to serve rural patients in Canada.[20] Recently, a Chinese group performed a series of successful demonstration "ultra-remote" (over 3,000 km distant) telesurgeries in pigs using a 5G network.[21]

NASA has long used telemedicine to monitor and treat astronauts and has been a major contributor to the development of terrestrial telemedicine. The COVID 19 pandemic has only highlighted and accelerated this transition. As a successor to the Integrated Medical and Behavioral Laboratories and Measurement Systems program, the Space Technology Applied to Rural Papago Advanced Health Care and NASA integrated astronaut care with rural health care.[22] Subsequently NASA was able to use telehealth to assist in two natural disasters, the earthquakes in Mexico City and Armenia.[23]

Recently, the wisdom of the deployment of diagnostic (and therapeutic) ultrasound to the International Space Station was proven when a deep-vein thrombosis was diagnosed and mitigated using an anticoagulant regiment.[24] However, even though remote cooperative telesurgery is feasible terrestrially, transmission delays beyond ~500 milliseconds make it unworkable beyond near earth orbit.[25] An alternative to the eventuality of an emergency surgery in space is to advance proper surgical robotics with specific qualities fit for long-term space exploration. Thus, we have been working on the development of low-mass, mini-surgical robots with surgical capability for long-duration missions.[17] Our existing small, lightweight, low-power miniature robots perform multiple essential tasks in one design including hemostasis, fluid management, suturing for traumatic wounds, and are fully insertable for internal surgical procedures. Capabilities of flight surgeons are necessarily limited, therefore for long-duration occupation of space, some level of autonomous medical capability will ultimately be key. Libraries of surgical procedures, residing on virtual reality (VR), or mixed reality training platforms will require human/machine interactive teaming with semi-autonomous surgical robots. A VR surgical trainer would grant spaceflight crew the capability for continued practice using a library of simulated subtasks and complete surgical procedures that would enable scheduling of skill acquisition and retention during long-duration missions and would provide a virtual assistant for emergent surgeries. These capabilities will have to be enabled with minimal ground-based guidance by incorporating autonomous and smart technology systems into the robots.

Recent advances in deep learning and artificial intelligence have demonstrated that complex, multistep tasks (e.g., self-driving vehicles) can be performed autonomously. However, applications of deep learning schema to automating surgical tasks are at least an order of magnitude more difficult than many current applications of deep learning to such domains as image identification or language recognition. The surgical environment is not only deformable in three dimensions, but also highly reflective and subject to changes in wavelength due to bleeds, vascular, and respiratory changes. Tissue interactions with surgical tools can rapidly and radically change the shape, color, and conformation of tissue, making recognition of the current state of the surgical field and appropriate automatic response a significant challenge. In addition, surgical tasks are happening concurrently with feedback from the surgical field that must be recognized and responded to by the autonomous robot in real time. Just as autonomous vehicle technology has developed hierarchically, we envision evolving levels of autonomous surgery development:

Level 0: Current technology. A surgical robot's movement is directly controlled by the surgeon, using an input device.

Level 1: Basic safety features. The surgical robot's tools can be stopped or slowed down automatically by a computer system that analyzes video and torque data from the robot, while considering parameters of the surgery input by the surgical team.

Level 2: Partial autonomous actuation. While the surgical robot's tools are still guided directly by the surgeon using controllers, the robot can actuate the tools to perform basic tasks, such as performing depth-controlled incisions or grasping tissue with correct forces.

Level 3: Surgeon-guided actuation. The robot is no longer directly controlled using a traditional input controller. Rather, the surgeon guides the robot's actions using a touch screen, pen input, VR headset, or other decoupled controller. The surgeon provide high-level instructions—like which tissue to excise, what path a cautery or suture line should follow—and the robot executes these instructions.

Level 4: Full autonomy. The surgeon instructs the robot which procedure to implement, and the robot is responsible for the surgery. The surgeon intervenes if complications arise.

The current study focuses on level 2 low-level development of semi-autonomous capability in medical robotics, specifically using machine learning techniques for robot vision detection of touch and force-detection using machine learning and waveform analysis. This basic form of measurement is essential to developing a system that can perform primitive surgical tasks, including depth-controlled incision, suturing, cautery, and grasping.

In summary, the potential need for an emergent surgery during long-term space missions is essential. Our study focuses on task automation surgery and on the development of semi-autonomous capability in medical robotics that could help make surgery safer through the prevention of collision and iatrogenic injury, increasing the crew medical capabilities.

We are on a long mission, (a) to develop a suite of low-mass, low-power robots capable of multiple internal and external surgical and medical tasks for long-duration missions, (b) to develop semi-autonomous capability in these robots, and (c) to understand how to build capable human/robot teams for surgery in space. To prepare for the probability of an emergency surgery during space flight, it is essential that surgical robot capabilities be further developed and automated.

METHODS

To achieve semi-autonomous capabilities, force-detection is a critical step. The approaches to force-detection used in our study can be separated into two categories. The first one uses visual feedback from the robot to predict events that correspond to physical contact between the robot and tissue in the operating environment. The second approach measures the motor current waveform used to drive the robot arms and uses deep learning to predict the amount of force being applied by the robot. The following sections describe each method.

Visual Contact Detection Using a Pixel-To-Pixel Deep Neural Network

Visual Contact Detection

A pixel-to-pixel fully convolutional neural network estimates contact between the robot arm and tissue. This network is generally derived from the U-net architecture proposed in.[26] The input image is a three-channel image captured from the perspective of the robot, as illustrated in the leftmost images in Fig. 1. While a single image capture does not convey motion in the scene, a series of image captures taken at different time points can be used to visualize both motion and deformation of objects in the scene. Therefore, instead of simply providing a single image to the network to estimate contact, the proposed method includes three stacked grayscale images from 0.5 seconds prior, 0.25 seconds prior, and the current time. In Fig. 1, the differences between these stacked images manifest

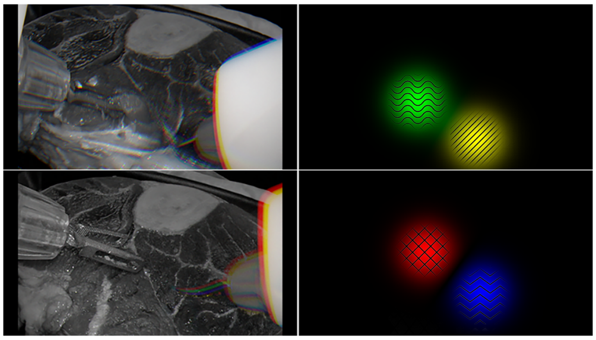

FIGURE 1. Illustration of the network inputs and the target feature outputs. As input the network concatenates images from 0.5 seconds prior, 0.25 seconds prior, and the current frame (all in grayscale) to get a single three-channel image capable of conveying motion and deformation within the scene. The output (on the right) is a four-channel output that combines local Gaussian kernels for end-effector detection with a -1 to 1 mapping for contact and no-contact events. Here, top and bottom kernels on the left illustrated by waves and grid patterns represent the spatial location of the left end-effector tip when it is contacting and not contacting with the tissue, respectively. The top and bottom right kernels illustrated by diagonal lines and sawtooth patterns represent the locations of the right end-effector tip in contact and no-contact scenarios, respectively. In the top example, the left end-effector is grasping the tissue while the right end-effector is pressing firmly into the tissue. In the bottom example, neither end effector is contacting the tissue.

as chromatic artifacts where the color indicates the direction of motion.

The output of the network is a four-channel feature space that encodes both the location of the end-effectors and a numerical method for representing contact or no contact. The first two channels produce Gaussian kernels at the locations of the left and right end-effector tips, respectively. The third and fourth channels encode contact/no-contact events numerically between -1 and 1 at the locations of the left and right end-effectors, respectively. Fig. 1 illustrates a colorized version of the four-channel feature space, where the green and red kernels indicate the location of the left end-effector and the yellow and blue kernels indicate the location of the right end-effector. Green and yellow, in this case, correspond to contact events where the third and fourth channel of the feature space would be encoded with a 1. Red and blue are no-contact events that correspond to encodings of -1 in the third and fourth channel.

The reason for separating the location from contact/no-contact events is to orthogonalize the outputs of the network. Processing the output of the network involves two stages. First, the peaks in the first two channels are found by comparing the 3×3 max pooling output of the first two channels to their original values. If the max pooling output is equal to the max pooling input, this corresponds to a regional maximum. If this regional maximum is also greater than 0.5, this corresponds to the estimated location of the end-effector. Once this location is found, the third and fourth channels are sampled at this location to determine whether the end-effector is contacting the tissue. Lastly, the precise location in the image space of the end-effector is found using quadratic interpolation of the feature space maximum and its vertical and horizontal neighbors.

To train and evaluate the proposed neural network approach to contact detection, we captured and annotated three separate videos where the robot manipulated the tissue with its end-effectors. The videos and their properties are provided in Table I. Tissue types include beef steak, skin-on chicken breast, and chicken gizzards. These three types were chosen to represent muscle tissue, skin, and internal organs. They were also chosen due to their widely varying appearance, where beef steak and skin-on chicken are not highly reflective and chicken gizzards are smooth and highly reflective. During the videos, the tissues were manipulated using single end-effector operations like pushing, pulling, squeezing, and cutting. Together, the two end-effectors also performed pull and cut and spreading operations. Throughout the course of each video, the robot was moved along the surface of the tissue, which altered its appearance through physical manipulations.

To train the neural network, only the first half of each video was used. The second halves of the videos are reserved for evaluating the accuracy of the trained network. It is worth noting that each frame of video was annotated for contact/no-contact events, but only every 75th frame was used for identifying the location of the end-effectors.

Sensorless Force Estimation

To enhance visual contact touch detection with high-fidelity force measurement data, we propose using motor current as a sensorless predictor for the force applied to the surgical environment. The proposed method uses a trained long short-term memory recursive neural network (LSTM RNN) to estimate the output torque of a motor's shaft based on the electrical current waveforms of the motor. The estimated torque is directly proportional to the output force through the robot's physical geometry, which the system models based on existing joint angle sensors. A spinning motor consuming I amperes exerts a torque of $T = I\,k_T$ where k_T is the motor's torque constant. However, this formulation excludes the inefficiencies between the motor shaft and the rest of the robot. Miniature motors used on small in vivo surgical robots use gearboxes with substantial gear ratios—4,000:1 scaling is not uncommon.

In the presence of friction, these gear trains do not transfer 100% of the power from the motor to the output shaft. This means when a motor uses a certain amount of current to produce a torque, the actual torque produced by the output of the

TABLE I. A. Dataset and Annotation Parameters for the Three Videos Used to Train and Evaluate the Visual Contact Estimation Network; B. The Results of the Visual Contact Detection Method on the Annotated Dataset. Both Training and Testing Accuracy are Given so that the Degree of Overfitting Can Be Assessed. Note That, "No Touch" Events Occur More Often than "Touch" Events, so the Accuracies between 50% and 78% are Achievable by Simply Guessing "No Touch" for Every Frame. These Effectively Provided as a Lower-bound for Classification Performance

Video	A Frames	Left Touch	Right Touch	Left No Touch	Right No Touch	B Training Left	Training Right	Testing Left	Testing Right
Beef Steak	37,401 (10.39 minutes)	18,600 (50%)	11,766 (31%)	18,801 (50%)	25,635 (69%)	94%	90%	90%	90%
Skin-On Chicken Breast	59,758 (16.60 minutes)	16,922 (28%)	13,092 (22%)	42,836 (72%)	46,666 (78%)	92%	92%	88%	86%
Chicken Gizzards	55,054 (15.29 minutes)	14,756 (27%)	17,323 (31%)	40,298 (73%)	37,731 (69%)	87%	87%	88%	87%

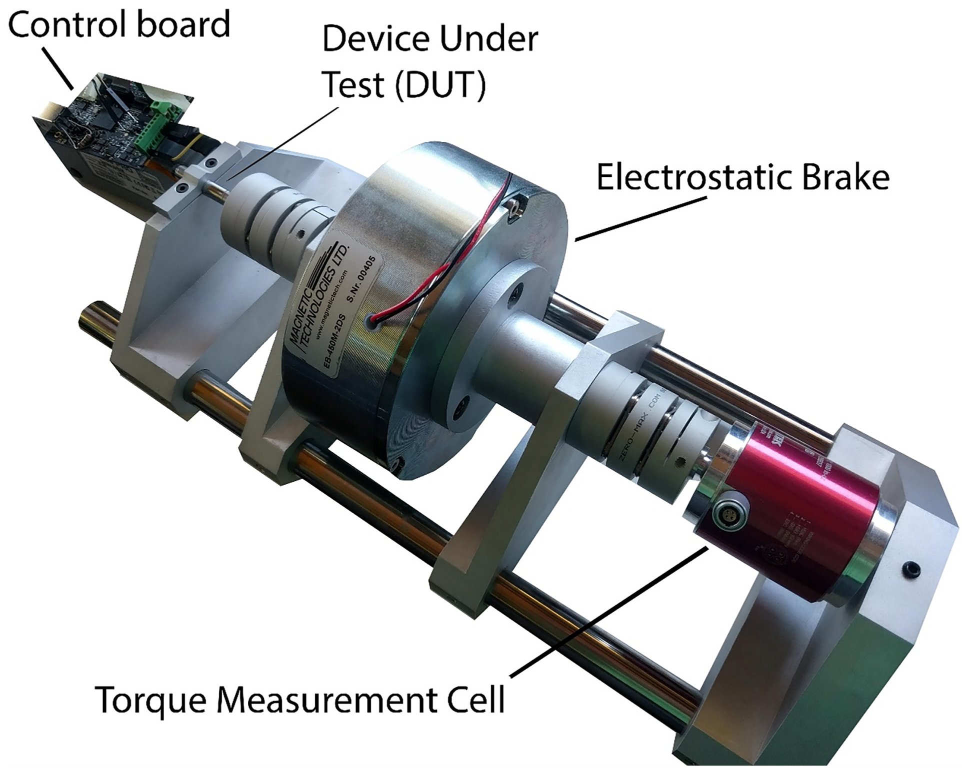

FIGURE 2. The dynamometer and control board measures motor current waveforms and delivered torque.

gear train can vary considerably depending on many factors, including gear meshing, lubricant temperature, particulate contamination in the gearbox, and manufacturing tolerance issues. The amount of efficiency drop caused by these factors is not constant (even for a particular unit) and cannot be parameterized easily.

Rather than attempting to model this efficiency in a forward fashion, we implement an LSTM RNN that can learn the relationship between motor current waveforms and output torque—possibly considering other inputs, like absolute output shaft position, temperature, humidity, age of the motor, a one-time factory calibration, etc.

This initial work focuses on building a test bed to begin to train the LSTM RNN. We created a dynamometer designed specifically for programmatically applying dynamic loads to a motor and measuring—with high precision—the output torque delivered (Fig. 2). The dynamometer uses 16-bit analog to digital converters for measuring motor current with a resolution of 15 μA, plus a 24-bit analog to digital converter for measuring output torque at a resolution of 417 nNm torque, and the system can capture these data at 500 kHz with more than 100 dB of signal-to-noise ratio.

For sensorless force estimation, the work covered here attempts to classify time-series electrical current waveforms, captured at 1.3 million samples per second, into motor torque output predictions. The measured motor was a Maxon EC12-series 8 mm brushless motor with a 1,024:1 gearbox.

RESULTS

The accuracy of visual contact detection is evaluated using the second half of the videos listed in Table I, which were not used for training the network. The results of the evaluation are also given in Table I. Regardless of tissue type, the accuracy is nearly 90% for contact/no-contact estimation. Furthermore, the difference between the training set performance and testing set performance is, at its maximum, 6%. In some cases, such as for chicken gizzards, the testing accuracy is better than the training accuracy.

Figure 3 illustrates the relationship of average current consumed by the motor to the output torque it produces. Due to static friction, it takes an average of at 150 mA of current just to get the shaft to start to spin (with no braking applied), and once the static friction is overcome and the motor starts spinning, the motor can start to develop torque with only minimal current consumption increase. The wide variance coupled with near-vertical slope of the data in this part of the plot illustrates the challenges of predicting output torque from average motor current. One input value—current—must correlate with a range of output torques. Most of this friction comes from the high-gain gearbox, though bearing friction in the dynamometer itself is also a contributor. Our instrument approaches 90% efficiency in the midband under a torque load of approximately 1 Nm and current consumption of approximately 200 mA, but the efficiency drops as current increases further and ohmic loss in the motor windings overwhelms the

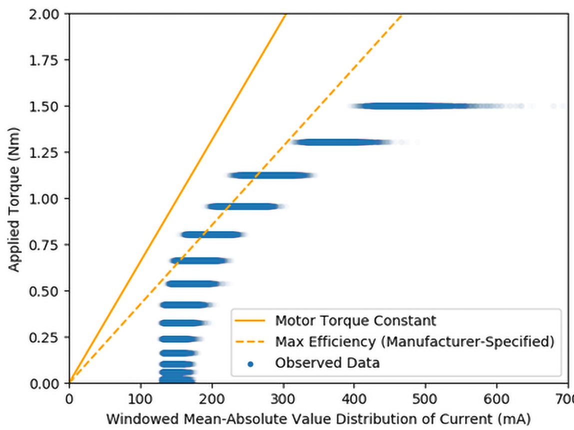

FIGURE 3. Ten-thousand instances of various motor current waveform sample windows plotted against the ground truth torque measured. The solid line illustrates the motor's torque constant; if the gearbox were 100% efficient, all sample points from the observed data would lie on the line. The dashed line is the maximum efficiency of the gearbox, as rated by the manufacturer. If the gearbox's efficiency were constant, all sample points would lie on the dotted line.

gains in torque. There is significant variance among motor current measurements for each applied torque value, and these measurements often overlap. This means that looking at windows averages of motor current time series is insufficient for predicting torque.

The LSTM RNN trained on 80% of the raw time-series data over several thousand epochs, and then evaluated against the remaining 20% ground truth data. Fig. 3 shows the output of the LSTM RNN during one time series. Note that the initial predicted current is quite poor, but after approximately 200 samples (~150 µs), the LSTM RNN converges to the correct torque value.

The LSTM RNN's time-series analysis predicted large torques with remarkable precision but struggled to predict small torque values from motor current. Further investigations—including integrating the previously mentioned additional data sources into the LSTM RNN model—will attempt to address these shortcomings.

DISCUSSION

Our preliminary data comprised a visual contact detection accuracy average greater than 90% for the training set and 80% for the testing set, providing feasibility of autonomous surgical tasks. Overall, the results indicate that even a small dataset is capable of being used to develop a visual contact estimation method for surgical robots. For implementation in a functional surgical platform, we expect that contact detection should be closer to 99%, as unintended physical contact can cause tissue damage and compromise the patient's safety. A final solution would likely include a multimodal sensing platform that combines inputs from visual and motor current feedback to achieve maximum fidelity.

While these results demonstrate that deep learning can achieve impressive accuracy in terms of classifying "touch"/"no-touch" events from single-camera video, this classification task is particularly well-suited to depth imaging either from active depth sensing or stereo reconstruction. Either of these imaging modalities would likely provide more useful inputs when texture deformation is difficult to discern from a single perspective. However, time-of-flight sensors at this scale are not currently available and stereo reconstruction in highly reflective environments presents considerable computer vision challenges.

Future directions include the combination of contact detection with estimation of applied forces, in addition to the recognition of binary "touch"/"no-touch" states. We also plan to build deep network models on top of touch/contact detection to perform primitive surgical tasks, including depth-controlled incision, suturing, cautery, and grasping. The outcomes demonstrated in this study are just one of the steps within the complex long-term work to provide autonomous surgical capabilities for long-term missions.

FUNDING SOURCES

This work was supported by a grant from the University of Nebraska System Science Collaboration Initiative and by the University of Nebraska Center for Advanced Surgical Technology.

REFERENCES

1. United States Space Force: United States space force: Available at https://www.military.com/space-force; accessed November 27, 2019.
2. Green PS, Hill JW, Jensen JF, Shah A: Telepresence surgery. IEEE Eng Med Bio Mag 1995; 14(3): 324-9.
3. Rosen J, Hannaford B: Doc at a distance. IEEE Spectr 2006; 43(10): 34-9.
4. Jayne D, Pigazzi A, Marshall H, et al: Effect of robotic-assisted vs conventional laparoscopic surgery on risk of conversion to open laparotomy among patients undergoing resection for rectal cancer: the ROLARR randomized clinical trial. JAMA 2017; 318(16): 1569-80.
5. Rentschler ME, Farritor SM, Iagnemma KD: Mechanical design of robotic in vivo wheeled mobility. J Mech Des 2007; 129(10): 1037-45.
6. Frazier RM, Carter-Templeton H, Wyatt TH, Wu L: Current Trends in robotics in nursing patents-A glimpse into emerging innovations. Comput Inform Nurs. 2019; 37(6): 290-7. PMID: 31135470.
7. Garcia P, Rosen J, Kapoor C, et al: Trauma Pod: a semi-automated telerobotic surgical system. Int J Med Robot 2009; 5(2): 136-46.
8. Dehghani H, Sun Y, Cubrich L, Oleynikov D, Farritor S, Terry BS: An optimization-based algorithm for trajectory planning of an under-actuated robotic arm to perform autonomous suturing. IEEE Trans Biomed Eng 2020; Epub ahead of print. PMID: 32946377.
9. Montidoro TA, Burgess JE, Antaki JF: Characterizing pressure and flow rate for aqueous immersion surgery. Surg Innov 2016; 23(1): 36-41.
10. Hayden JA, Pantalos GM, Burgess JE, Antaki JF: A hermetically sealed, fluid-filled surgical enclosure for microgravity. Aviat Space Environ Med 2013; 84(12): 1298-303.
11. Kirkpatrick AW, Ball CG, Campbell M, et al: Severe traumatic injury during long duration. J Am Coll Surg 2002; 194(6): 802-12.
12. Campbell MR: A review of surgical care in space medical problems. Environ Med 1998; 42(2): 83-94.
13. Grigoriev AI, Svetaylo EN, Egorov AD: Manned interplanetary missions: prospective spaceflight: light years beyond ATLS. J Trauma Manag Outcomes 2009; 3(1): 3-4.

14. Panesar SS, Ashkan K: Surgery in space. Br J Surg 2018; 105(10): 1234-43.
15. Drudi L, Ball CG, Kirkpatrick AW, Saary J, Grenon SM: Surgery in space: where are we at now? Acta Astronaut 2012; 79: 61-6. PMID: 23990690; PMCID: PMC3752909.
16. Hodkinson PD, Anderton RA, Posselt BN, Fong KJ: An overview of space medicine. Br J Anaesth 2017; 119(Suppl 1): i143-53.
17. Reichenbach M, Frederick T, Cubrich L, et al: Telesurgery with miniature robots to leverage surgical expertise in distributed expeditionary environments. J Mil Med 2017; 182(Suppl 1): 316-21.
18. George EI, Brand TC, LaPorta A, Marescaux J, Satava RM: Origins of robotic surgery: from skepticism to standard of care. JSLS 2018; 22(4): e2018.00039.
19. Marescaux J, Leroy J, Gagner M: Transatlantic robot-assisted telesurgery. Nature 2001; 413(6854): 379-80.
20. Anvari M, McKinley C, Stein H: Establishment of the World's first telerobotic remote surgical service: for provision of advanced laparoscopic surgery in a rural community. Ann Surg 2005; 241(3): 460-4.
21. Zheng J, Wang Y, Zhang J, Guo W, et al: 5G ultra-remote robot-assisted laparoscopic surgery in China. Surg Endosc 2020; 34(11): 5172-80. Epub 2020 Jul 22. PMID: 32700149.
22. Freiburger G, Holcomb M, Piper D: The STARPAHC collection: part of an archive of the history of telemedicine. J Telemed Telecare 2007; 13(5): 221-3.
23. Simpson A, Doarn C, Garber S: A brief history of NASA's contribution to telemedicine. Available at https://history.nasa.gov/NASA telemedicine-briefhistory.pdf; accessed September 28, 2020.
24. Auñón-Chancellor SM, Pattarini JM, Moll S, Sargsyan A: Venous thrombosis during spaceflight. N Engl J Med 2020; 382(1): 89-90.
25. Korte C, Sudhakaran Nair S, Nistor V, Low TP, Doarn CR, Schaffner G: Determining the threshold of time-delay for teleoperation accuracy and efficiency in relation to telesurgery. Telemed J E Health 2014; 20(12): 1078-86.
26. Ronneberger O, Fischer P, Brox T: U-Net: convolutional networks for biomedical image segmentation. Medical image computing and computer-assisted intervention 2015; Available at https://arxiv.org/pdf/1505.04597.pdf; accessed April 9, 2020.